Journal of Applied Electrochemistry **30**: 269–275, 2000.

Mass transport in lithium-battery solvents

MARK W. VERBRUGGE[1], BRIAN J. KOCH[1] and ERIC W. SCHNEIDER[2]
[1]*General Motors Advanced Technology Vehicles, 1996 Technology Dr., Troy, Michigan 48007-7083, USA*
[2]*General Motors Research and Development Center, 30500 Mound Rd., Warren, MI 48090-9055, USA*

Received 15 April 1999; accepted in revised form 1 October 1999

Key words: batteries, lithium, lithium perchlorate, microelectrode, radiotracer

Abstract

We describe and implement a microelectrode procedure for the determination of important transport properties required for the evaluation of liquid electrolytes used in lithium-based batteries. Three solvents of interest (propylene carbonate, ethylene carbonate, and diethyl carbonate) and two lithium salts (lithium hexafluorophosphate and lithium perchlorate) are investigated. In addition, by combining microelectrode and radiometric analyses, we are able to characterize fully the transport phenomena in the nonaqueous solvent + salt systems. Thus a radiometric technique is used to monitor solvent transport, both under diffusion and current-passage conditions, and the solvent diffusion coefficient is reported as a function of salt concentration.

List of symbols

a	disk radius
c	salt concentration
d	diameter of transport channel (Figure 1)
D	diffusion coefficient
F	Faraday constant
i	current density
L	length of transport channel (Figure 1)
N	species flux
$\mathcal{N}$	number of propylene carbonate molecules coordinating a lithium cation
t	time
t_0	transference number with respect to the solvent velocity
V	reservoir volume (Figure 1)
z	charge number

Subscripts and superscripts

avg	average
PC	propylene carbonate
*	radiotracer species
−	anion
+	cation
0	solvent
∞	far from the electrode surface

1. Introduction

For electric and hybrid vehicle batteries, the energy available under most discharge conditions is limited primarily by the capacity of the electrode materials and the thermodynamic potential difference between the two electrodes, while the power capability is influenced greatly by irreversible processes, such as intraparticle and electrolyte-phase diffusion, interfacial (electrochemical) reaction, and ionic migration. Cell-chemistry models [1–7] have shown that for reasonably small sizes of active-material particles, i.e., less than a few microns in characteristic size, both intraparticle and electrochemical reaction resistances [8, 9] can be substantially reduced, leaving electrolyte-phase transport resistance to limit the power-delivery rate.

In order to quantify the transport limitations in electrolytes of immediate interest for lithium battery applications, characterization procedures are described and implemented. Solutions containing either lithium hexafluorophosphate ($LiPF_6$) or lithium perchlorate ($LiClO_4$) salts in solvents of propylene carbonate, propylene carbonate + ethylene carbonate, or ethylene carbonate + diethyl carbonate are analyzed. In addition, the diffusion of ^{14}C tagged propylene carbonate is determined as a function of $LiClO_4$ concentration, yielding information useful for the elucidation of electrolyte-phase transport phenomena and specific solvent-salt interactions.

The scope of this work is to describe and implement procedures for the determination of important transport properties. Because actual lithium battery systems utilize a mixture of solvents and various salts, and there is no uniform agreement as to the optimal solvent + salt system, it is beyond the scope of this work to characterize the entire range of solvent + salt systems of immediate technological significance. For this reason, only the better-understood lithium per-

chlorate + propylene carbonate system is studied in detail.

2. Experimental

2.1. *Chemicals*

All salts and solvents on which we report were obtained from Fluka and were greater than 99% purity. The $LiClO_4$ was dried in a heated, evacuated antechamber at 100 °C, and a temperature of 60 °C was used for the $LiPF_6$. Solutions were made with vacuum distilled solvents; the distillation procedure and apparatus are described elsewhere [10] and correspond closely to those detailed by Jasinski and Kirkland [11]. Lithium (Foote Mineral, 99.99%) was used to construct the counter/reference electrode. (The counter and reference electrodes are one and the same for the microelectrode experiments.) All experiments were carried out in a Vacuum Atmospheres glove box fed with 99.999% argon gas (Scott Speciality Gases). Provisions were made to remove trace amounts of oxygen and water.

Propylene carbonate with radioactive ^{14}C incorporated at the carbonyl position was employed as the radiotracer species (Amersham). Radio-gas chromatography indicated a 97.7% radiochemical purity of the tracer. The initial radiotracer solution was diluted to a 6 ml volume by the addition of untagged propylene carbonate. This diluted stock solution, having a specific activity of 0.83 mCi ml^{-1}, was maintained at −20 °C in a sealed container prior to usage.

2.2. *Instrumentation*

The electrochemical cells were controlled by a Bioanalytical Systems 100B Electrochemical analyzer. Platinum 38 μm radius electrodes, sealed in glass, were constructed and prepared using standard methods [12, 13]. References [14, 15] describe related analyses of polymer electrolyte systems. All lithium experiments were done in a Faraday cage within the glove box. Radiometric assays of the ^{14}C solutions were performed using a Packard Tri-Carb CA2000 Liquid Scintillation Analyzer.

2.3. *Radiometric measurements*

An aliquot of the radiotracer stock solution (0.06 to 0.5 ml, depending on the anticipated diffusion or transport rate) was transferred to the 'hot' reservoir of the radiotracer cell, shown schematically in Figure 1. Due to the cell design and construction, transport resistance is confined primarily to the channel, and the well-stirred reservoirs offered no significant resistance to propylene carbonate transport. The simultaneous deposition of an equal volume of untagged solution was made to the 'cold' reservoir of the cell to eliminate flow through the channel due to a differential in liquid levels. Samples from both reservoirs (0.1 ml) were removed simultaneously and at regular time intervals for liquid-scintillation (LS) analysis. Depending on the amount of radiotracer stock solution employed, sample volumes from the hot reservoir were reduced by a factor of 10 prior to analysis. (This procedure was used to reduce sample activities so that dead-time counting losses during the radiometric assay were not significant.) The samples were transferred into 15 ml aliquots of Instagel-XF LS cocktail (Packard) in LS counting vials. Samples were counted until statistical uncertainties were better than 0.5%, or for a maximum of 60 min. The quench rate of each sample was determined from the Compton spectrum induced by an external ^{133}Ba source. After background subtraction, observed count rates were converted to ^{14}C disintegration rates by corrections from quench standards (Packard).

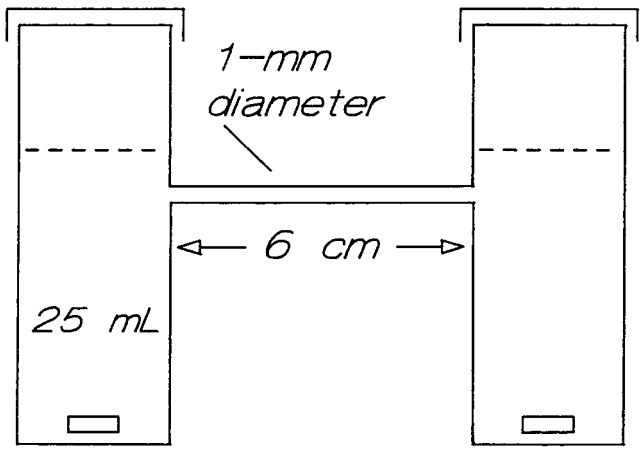

Fig. 1. Schematic illustration of the cell used for the radiotracer experiments. Both reservoirs were well stirred.

3. Chronoamperometry analyses

The electrochemical experiments discussed concern transport-controlled conditions associated with the reaction

$$Li^+ + e^- \rightleftharpoons Li^0 \tag{1}$$

The governing equations to be described below are appropriate for the treatment of a concentrated binary electrolyte; a general overview of phenomenological relations and resulting conservation equations can be found elsewhere [16].

3.1. *Governing equations for transport characterization*

The governing equations that describe the transient, two-dimensional problem for the microdisk system consistent with our experimental conditions are [17, 18, 19]

$$\frac{\partial c}{\partial t} = D\nabla^2 c \tag{2}$$

$$c = c^{\infty} \quad \text{initially} \tag{3}$$

$$c = c^{\infty} \quad \text{far from disk electrode} \tag{4}$$

$$c = 0 \quad \text{on the disk, and} \tag{5}$$

$$\nabla c \cdot \underline{n} = 0 \quad \text{on the insulator surrounding the disk} \tag{6}$$

where D refers to the diffusion coefficient of the salt

$$D = \frac{D_{+0}D_{-0}(z_+ - z_-)}{z_+D_{+0} - z_-D_{-0}}$$

t denotes time, c^{∞} represents the initial and bulk-solution concentration of salt, and $\underline{n}$ is the surface unit-normal vector pointing into solution. Thus the salt diffusion coefficient, D, results from a combination of diffusion coefficients reflecting cation-solvent (subscript $+0$) and anion-solvent (subscript -0) interactions. Upon solving these equations for the salt concentration c, the component of the local current density normal to the disk surface, i, can be calculated from

$$\frac{i}{F} = -\left(\frac{D}{1 - t_+^0}\right)\nabla c \cdot \underline{n} \tag{7}$$

where F denotes Faraday's constant, the lithium cation transference number t_+^0 (with respect to the solvent velocity) is given by

$$t_+^0 = \frac{z_+D_{+0}}{z_+D_{+0} - z_-D_{-0}}$$

and $t_+^0 + t_-^0 = 1$. The average current i_{avg}, which is to be compared with experiments for the measurement of D and t_+^0, is given by

$$i_{\text{avg}} = \frac{1}{\pi a^2}\iint_{\text{A}} i \, \text{dA}$$

These governing equations result from concentrated-solution theory if the propylene carbonate solvent is immobile and the solvent concentration as well as the ionic transport coefficients are invariant over the range of concentrations investigated [13]. For the steady-state condition, $\nabla^2 c = 0$, and [12, 13]

$$i_{\text{avg}} = -\frac{4F}{\pi a}\left(\frac{D}{1 - t_+^0}\right)c^{\infty} \quad (t \to \infty) \tag{8}$$

For short times the results of Aoki and Osteryoung [18, 19] can be used to express the average current density as

$$i_{\text{avg}} = -\frac{F}{a\sqrt{\pi}}\left(1 + \frac{a}{\sqrt{tD}} + 0.094\frac{8}{a\pi}\sqrt{tD}\right) \times \left(\frac{D}{1 - t_+^0}\right)c^{\infty} \quad (tD\ a^{-2} \text{ small}) \tag{9}$$

This equation is sufficiently accurate for $tD/a^2 \leq 0.1$ [17, 18, 19]. Thus steady-state transport-limited current plateaus corresponding to the current decay after a potential step to the transport-limited condition can be used to determine t_+^0 by means of Equation (9) and the measured quantity $D/(1 - t_+^0)$. The only remaining electrolyte-phase physicochemical parameter required for the mathematical simulation of batteries employing a binary electrolyte [1–6] is the ionic conductivity, which is easily measured and well known [20, 21] for the solvent–salt systems investigated herein.

3.2. *Pseudo steady-state experiments*

For the current-potential traces shown in Figure 2, the potential of the microdisk electrode was scanned linearly with time, from 0 V vs. Li to more negative values, at a scan rate of 25 mV s^{-1}. Because of the low $LiPF_6$ concentration, 0.05 M, the deposition current density in accordance with Equation (1) is sufficiently low to preclude substantial deposit growth that could lead to a change in the electrode geometric area, and well-defined limiting current plateaus can be obtained. As has been reported in previous studies, no evidence of solvent reduction was found prior to the clear onset of $LiPF_6$ transport limitations. Since the Pt disk was initially devoid of lithium deposit, a finite cathodic (deposition) current was observed immediately upon scanning from 0 V (cf. Figure 3 of [12]).

The results shown in Figure 2 indicate that the quantity $D/(1 - t_+^0)$ appearing in Equation (8), which can be applied to simulate the limiting-current plateau, is the same for propylene carbonate + 0.05 M $LiPF_6$ and 1:1 by weight propylene carbonate + ethylene carbonate solvents of the same dilute $LiPF_6$ concentration. In contrast, the less viscous diethyl carbonate allows for faster salt diffusion, which explains the larger magnitude of the limiting-current plateau for the ethylene carbonate + diethyl carbonate solvent mixture

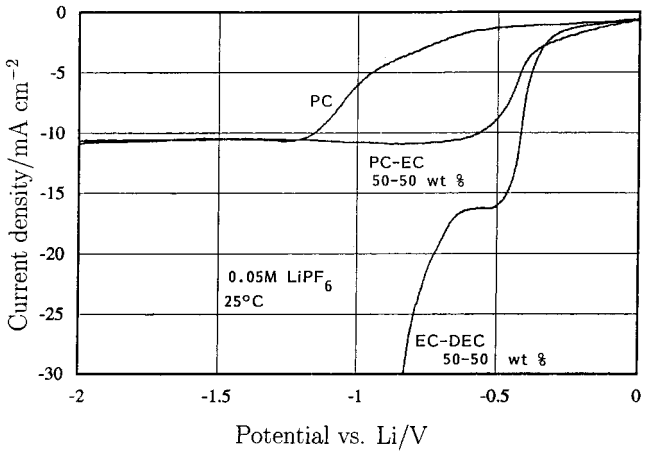

Fig. 2. Experiments for the determination of steady-state transport-limited currents. The potential was scanned linearly with time, from 0 V vs. Li to more negative values, at a scan rate of 25 mV s^{-1}. A 0.05 M $LiPF_6$ salt concentration was employed, and the various solvents are indicated (PC: propylene carbonate, EC: ethylene carbonate, DEC: diethyl carbonate).

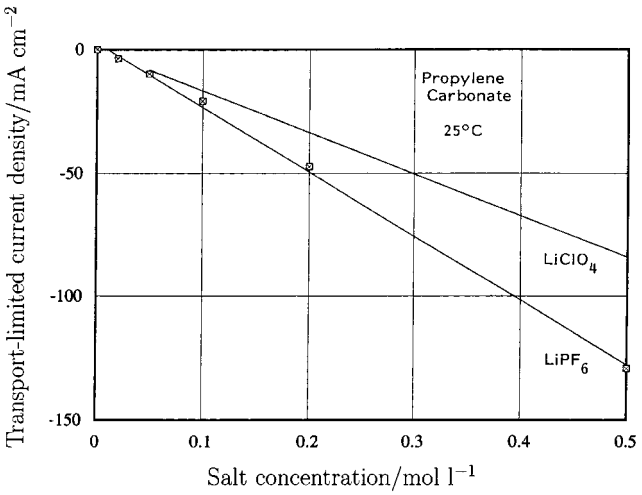

Fig. 3. Concentration dependence of the limiting-current plateau for $LiPF_6$ in propylene carbonate. The transport-limited currents were obtained from current-potential curves similar in appearance to those shown in Figure 2 for the propylene carbonate + $LiPF_6$ solution. Also displayed is the published curve for $LiClO_4$ in propylene carbonate [13].

relative to that of the propylene carbonate + ethylene carbonate mixture. In addition, the small potential range (−0.5 to −0.6 V) associated with the limiting-current plateau for the diethyl carbonate + ethylene carbonate solvent mixture indicates that the lower-molecular-weight, linear carbonate is less stable to reduction then either of the heavier cyclic carbonates.

The concentration dependence of the limiting-current plateau for $LiPF_6$ in propylene carbonate is displayed in Figure 3 (0 to 0.5 M) along with the published curve relating the transport-limited current density to salt concentration for propylene carbonate + $LiClO_4$ solutions [13]. As was found for propylene carbonate + $LiClO_4$ solutions up to 1 M, the transport coefficients D and t_+^0, which determine the slopes of the curves shown in Figure 3, are to good approximation independent of salt concentration over the range of study. The values of $D/(1-t_+^0)$ for the various solutions are stated in Table 1 and were taken from data shown in Figures 2 and 3.

3.3. *Potential-step experiments*

Upon stepping the potential to large, negative values, the surface concentration of the lithium salt tends to zero immediately, and Equation (9) can be used to determine t_+^0 and D, the quantity $D/(1-t_+^0)$ being obtained previously as described above. Results for propylene carbonate + 0.05 M $LiClO_4$ are shown in Figure 4. The data are represented by symbols. If the first and last terms of the quantity $(1+(a/\sqrt{tD})+0.094(8/a\pi)\sqrt{tD})$ in Equation (9) are dropped, the Cottrell equation results [17]. Curves A and B shown in Figure 4 represent calculations that are obtained with the first two terms and all three terms, respectively. It is important to note that in fitting the transference number to the data shown in the lower plot of Figure 4, both the slope and magnitude of the current vs. $1/\sqrt{t}$ relation are sensitive to the lone fitted parameter D, which lends strong support to the concept that the overall approach taken in this treatment is fundamentally correct. The fitted transference number and salt diffusion coefficient are:

$$\left.\begin{aligned} t_+^0 &= 0.44 \\ D &= 2.9\times10^{-6}\ \text{cm}^2\ \text{s}^{-1} \end{aligned}\right\} \begin{aligned} &\text{Propylene carbonate} + LiClO_4 \\ &c_{LiClO_4} \le 1\ \text{M} \end{aligned}$$

The lithium ion transference number of 0.44 is in qualitative agreement with previous studies [22–24] in that the lithium cation, being more strongly solvated than the perchlorate anion [25] is part of a larger solvated complex and is represented by a lower trans-

Table 1. Values for the quantity $D/(1-t_+^0)$, appearing in Equation 8, for various solvent + salt systems

Solvent + salt system	$D/(1-t_+^0)$ cm^2 s^{-1}
Propylene carbonate + $LiPF_6$ and (1:1 wt. ratio) propylene carbonate, ethylene carbonate + $LiPF_6$	7.8×10^{-6}
Propylene carbonate + $LiClO_4$ [13]	5.2×10^{-6}
(1:1 wt. ratio) Ethylene carbonate, diethyl carbonate + $LiPF_6$	9.9×10^{-6}

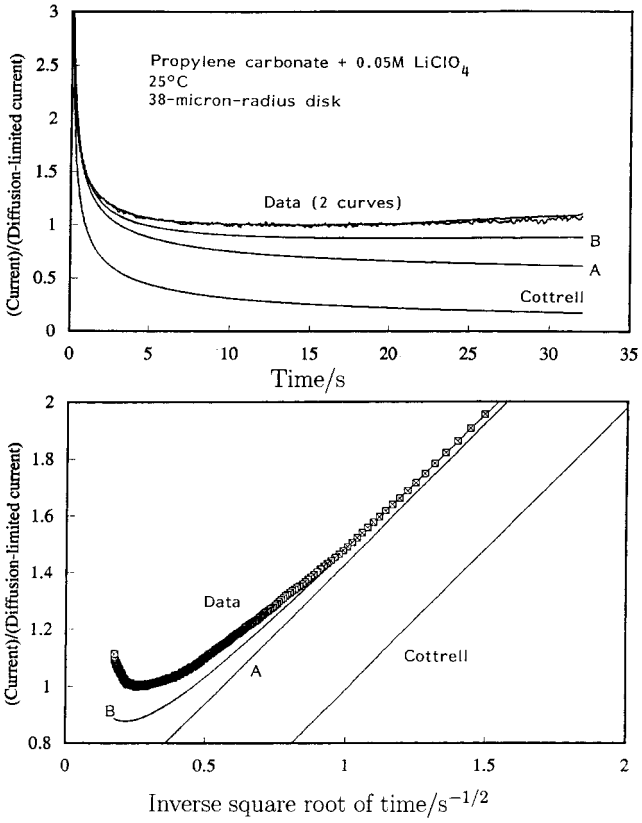

Fig. 4. Potential-step experiments. Upper panel: two experimentally obtained current-time traces and theoretical traces discussed in the context of Equation (9). Lower panel: dimensionless currents shown in the upper panel are plotted against $1/\sqrt{t}$.

ference number and ionic diffusion coefficient than the perchlorate anion. There is, however, a large difference in values reported for t_+^0, probably due to the difficulties associated with prior methods used to determine the transference number [26]. The measured salt diffusion coefficient of 2.9×10^{-6} cm^2 s^{-1} is very close to that reported by Sullivan et al. [27] of 2.6×10^{-6} cm^2 s^{-1} for a 1 M $LiClO_4$ + propylene carbonate solution. While it is possible to identify studies reporting values for either t_+^0 or D that are close to those reported here, there is a wide spread in the reported values [22, 24] and it is notable that the results reported in this work for t_+^0 and D were obtained with the same experimental set up and nominally at the same time.

The reproducibility of the potential-step experiments is indicated by the two data curves shown in the upper plot of Figure 4 being nearly identical. The smoother of the two data curves was obtained with a higher gain on the current amplifier. We attempted to perform the same experiment with $LiPF_6$, but effects perhaps related to nucleation and growth, as have been reported for fluoride-based lithium salts [28] precluded facile deposition initially, and Equation (9) could not be applied to treat the resulting data.

It is expected that neither the experimental results nor the theoretical curves shown in the lower plot of Figure 4 are particularly useful for longer times, i.e., for values of time greater than about 1 s, or, correspondingly, for values of $1/\sqrt{t}$ less than 1 s$^{-1/2}$. Equation (9), curve B, is valid only for short times, and the curves marked A and Cottrell represent progressive approximations to Equation (9). Long-time asymptotic solutions are reviewed and discussed elsewhere [29]. For intermediate times, numerical calculations are required [30–32]. With regard to the experimental data, the effects of deposit growth are identified clearly by the upturn in the measured current near a value of $1/\sqrt{t} = 0.25$ s$^{-1/2}$, or $t = 16$ s.

4. Radiometric analyses

4.1. *Mathematical relations for data analysis*

Propylene carbonate diffusion and transport during current passage are described in this section. A schematic of the radiotracer cell appears in Figure 1. The analysis to follow is consistent with the transport resistance being confined to the channel, as indicated in the Experimental section. For a detailed treatment of tracer diffusion experiments that includes the effects of both mutual and self-diffusion coefficients, see [33]. Such effects are generally of lower-order importance when large molecules are the tracer species [33, 34]; we shall assume that the dilute-solution treatment offered below is appropriate for propylene carbonate.

The pseudo steady-state flux N_* of tagged, and extremely dilute, propylene carbonate from the hot reservoir to the cold reservoir is given by

$$N_* = D_* \frac{c_*^{\text{hot}} - c_*^{\text{cold}}}{L} \tag{10}$$

where c_* denotes the concentration of the propylene carbonate radiotracer and D_* refers to the tracer diffusion coefficient. For the conditions of this work, $c_*^{\text{cold}} \ll c_*^{\text{hot}}$. A material balance on the cold-side reservoir of volume V yields

$$V \frac{\partial c_*^{\text{cold}}}{\partial t} = N_* \frac{\pi d^2}{4} = \frac{\pi d^2}{4} D_* \frac{c_*^{\text{hot}} - c_*^{\text{cold}}}{L} \tag{11}$$

Because $c_*^{\text{cold}} \ll c_*^{\text{hot}}$, $(\pi d^2/4)L/V \ll 1$, and $tD_*/L^2 \gg 1$, Equation (11) can be replaced with [35, 36]

$$\frac{c_*^{\text{cold}}}{c_*^{\text{hot}} t} = \frac{\pi d^2}{4V} \frac{D_*}{L} \tag{12}$$

We shall also provide data corresponding to current passage, conditions under which propylene carbonate solvates lithium cations that transport from an anodically dissolving lithium foil in the hot reservoir to the cold side containing a lithium-foil cathode. For the pseudo steady-state, we may treat the perchlorate anions within the channel as immobile, as they are not involved in the electrode reactions. Within the channel, the lithium flux at steady-state is given by i/F, where i refers to the cell current density based on the channel's geometric area (1 mA cm^{-2} in this work). We shall not attempt a quantitative analysis of the current-passage experiment, but it is helpful to suggest an approximate treatment to provide a basis for analyzing the data. In particular, if one assumes that the time period over which propylene carbonate molecules exchange into and out of solvation shells is large relative to the time it takes for lithium cations to transport across the channel, then the flux of tagged propylene carbonate from the hot reservoir to the cold reservoir can be approximated as

$$N_* = D_* \frac{c_*^{\text{hot}} - c_*^{\text{cold}}}{L} + \mathcal{N} \frac{c_*^{\text{hot}}}{c_{\text{PC}}} \frac{i}{F} \quad \text{(irreversible solvation kinetics)} \tag{13}$$

where $\mathcal{N}$ is the number of propylene carbonate molecules coordinating a lithium cation, and, based on an atomic weight of 102 g mol^{-1} and a density of 1.2 g cm^{-3} [37] the (untagged) propylene carbonate concentration c_{PC} in solution is 0.012 mol cm^{-3}. Thus to alter Equation (12) so as to incorporate this qualitative treatment of the current-passage experiment, D/L is replaced by $((D/L) + (\mathcal{N}/c_{\text{PC}})(i/F))$.

4.2. *Radiometric results*

The data shown in Figure 5 are characteristic of those collected for the diffusion studies; also shown in Figure 5

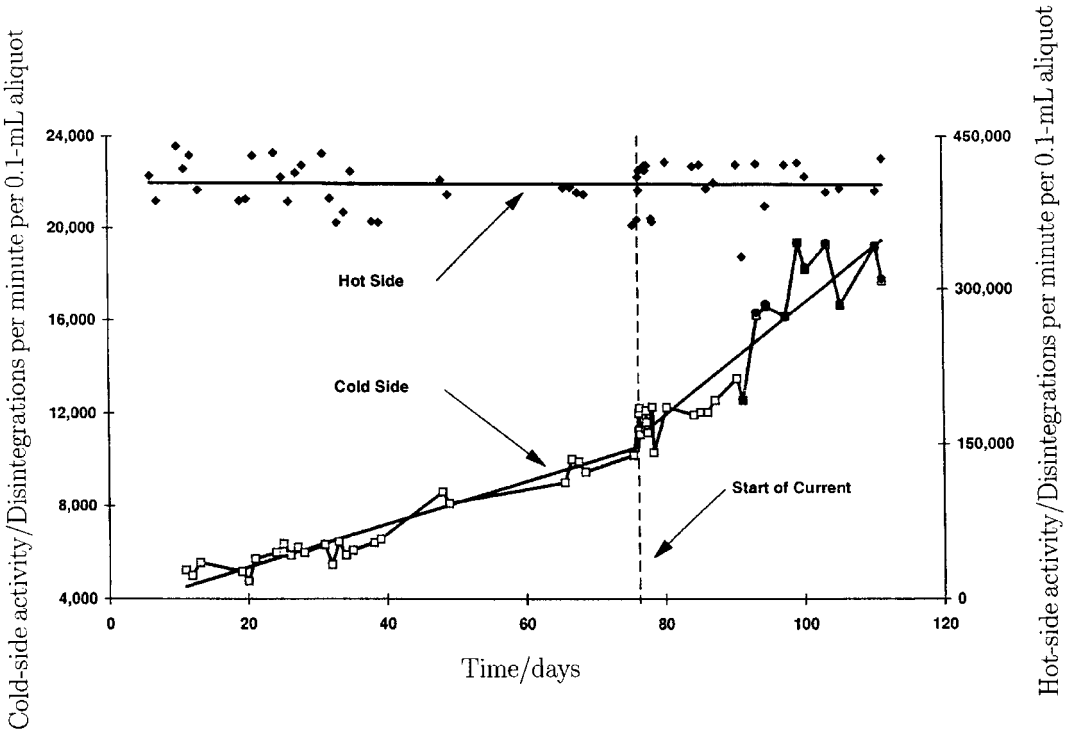

Fig. 5. Experimental data for the radiometric analysis. For the displayed data, an 8:1 molar ratio of propylene carbonate to $LiClO_4$ was employed. The data shown are characteristic of those collected for the propylene carbonate diffusion coefficients; also shown are the results for a 1 mA cm^{-2} current-passage experiment. Duplicate counts of the last 10 cold-side samples are shown to verify that the radiometric measurement errors are small compared to those of other sources, such as pipetting-aliquot variations and temperature changes over the experiment duration.

are the results for the one current-passage experiment that was conducted, which is discussed below. A number of features warrant discussion. First, we note that the hot-side concentration is large and invariant relative to that of the cold side, consistent with the approximation $c_*^{hot} - c_*^{cold} \approx c_*^{hot}$ used in deriving Equation (12). In keeping with the philosophy of presenting an untreated data set, the plotted cold-side activity corresponds to the disintegration per minute per 0.1 ml aliquot withdrawn, while the plotted hot-side activity corresponds to the disintegration per minute per 0.01 ml diluted aliquot withdrawn. Second, the duration of the experiment is quite long, $tD_*/L^2 \gg 1$, and the cold-reservoir disintegration per minute increases linearly with time. The two largest sources of error in the analysis were most likely pipetting irregularities and temperature fluctuations during the test. Of these, only the former can explain a decrease in the plotted activity vs. time. Third, we note that the cold-reservoir activities are well above the measured background (≈30 disintegrations per minute), and the subsequent counting of the aliquots yielded no significant differences in c_*^{cold}, as is indicated by the agreement between the two separate counts shown for the last 10 data points on the cold-side results of Figure 5. (For the results shown in Figure 5, the diffusion experiment was initiated after a previous experiment, and the disintegration per minute corresponding to zero time are large relative to that of background. The change in the measured disintegration per minute over the experiment duration, however, was two orders of magnitude greater than background.)

The first objective of the diffusion studies was to determine the propylene carbonate diffusion coefficient as a function of $LiClO_4$ salt concentration. Thus D_* is plotted against the $LiClO_4$ concentrations in Figure 6. The values of D_* shown in Figure 6 were obtained from disintegration per minute vs. time slopes, similar to the diffusion portion of the plot shown in Figure 5, for each indicated salt concentration, with Equation (12) applied to calculate D_*. For each data point, with the exception of that corresponding to pure propylene carbonate, the molar ratio of propylene carbonate to $LiClO_4$ is

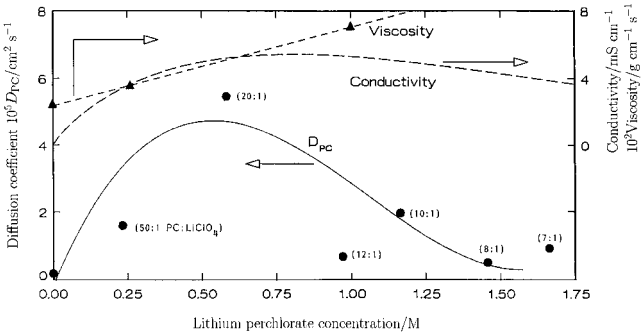

Fig. 6. Diffusion coefficient of tagged propylene carbonate along with the solution conductivity [20, 21] and viscosity [22]. The diffusion-coefficient values were obtained from disintegration per minute vs. time slopes similar to the diffusion portion of the plot shown in Figure 5 for each indicated salt concentration, with Equation (12) applied to calculate D_*. For each data point, with the exception of that corresponding to pure propylene carbonate, the molar ratio of propylene carbonate to $LiClO_4$ is specified in parentheses.

specified in parentheses. The mean value is 2.8×10^{-5} cm^2 s^{-1}, and, like the plotted ionic conductivity for propylene carbonate + $LiClO_4$ solutions [20, 21] D_* decreases for propylene carbonate to $LiClO_4$ ratios less than about 20, corresponding to salt concentrations above about 0.5 M. Increases in viscosity [22], which are also plotted in Figure 6, have been cited in attempts to explain the decrease in conductivity [20, 21] but it is not immediately clear why the quantity $D/(1 - t_+^0)$ does not show a similar decline for concentration between 0.5 and 1 M [13]. In addition, there is no firm explanation that can be offered to explain why D_* increases with $LiClO_4$ concentrations in dilute salt solution, although one can speculate that structure-forming mechanisms in pure propylene carbonate solutions may be disrupted upon the addition of salt, allowing for more mobile propylene carbonate. This speculation, however, does not readily explain the concurrent increase in solution viscosity.

The diffusion coefficient D_* corresponding to an 8:1 propylene carbonate to $LiClO_4$ ratio, 5×10^{-6} cm^2 s^{-1}, can be used along with the current-passage data shown in Figure 5 and Equation (13) to obtain a value of $\mathcal{N} \approx 2$. We would expect the actual cation solvation number to be larger than two for propylene carbonate + $LiClO_4$ solutions based on the properties of propylene carbonate [37] and we should expect the very approximate treatment embodied in the use of Equation (13) to underestimate the cation solvation number, as the treatment does not consider the exchange of propylene carbonate molecules into and out of a solvated complex.

5. Conclusion

The electrochemical data obtained and analyzed in this study constitute a robust interpretation of the $LiClO_4$ + propylene carbonate system. This assertion is based on (i) the unambiguous limiting current plateaus of large duration, (ii) the demonstrated reproducibility of the potential-step experimental data (upper panel, Figure 4), and (iii) the need to include higher order terms [18, 19] in the analysis of potential step data in order to capture both the slope and magnitude of the curve representing microdisk current versus inverse square root of time (lower panel, Figure 4). With regard to the last point, confidence in the analysis is clearly enhanced when the addition of higher-order terms leads successively to improved agreement between experimental and theoretical results. While the radiometric analysis shows clear trends in the variation of the diffusion coefficient of ^{14}C-tagged propylene carbonate with $LiClO_4$ concentration, and viscosity as well as other physical property data are available over the same range of salt concentrations [20, 21, 22] several unanswered questions remain; the data should, however, provide fertile grounds for solution-phase analysis required to unravel the underlying chemistry [25].

References

1. M. Doyle, T.F. Fuller and J. Newman, *J. Electrochem. Soc.* **140** (1993) 1526.
2. T.F. Fuller, M. Doyle and J. Newman, *J. Electrochem. Soc.* **141** (1994) 1.
3. T.F. Fuller, M. Doyle and J. Newman, *J. Electrochem. Soc.* **141** (1994) 982.
4. M. Doyle, J. Newman and J. Reimers, *J. Power Sources* **52** (1994) 211.
5. M. Doyle, T.F. Fuller and J. Newman, *Electrochimica Acta* **39** (1994) 2073.
6. M. Doyle, J. Newman, A.S. Gozdz, C.N. Schmutz and J-M. Tarascon, *J. Electrochem. Soc.* **143** (1996) 1890.
7. M.W. Verbrugge, *J. Electrostatics* **34** (1995) 61.
8. M.W. Verbrugge and B.J. Koch, *J. Electrochem. Soc.* **143** (1996) 600.
9. M.W. Verbrugge and B.J. Koch, *J. Electrochem. Soc.* **146** (1999) 833.
10. M.W. Verbrugge and B.J. Koch, *J. Electrochem. Soc.* **143** (1996) 24.
11. R.J. Jasinski and S. Kirkland, *Anal. Chem.* **39** (1967) 1663.
12. M.W. Verbrugge and B.J. Koch, *J. Electroanal. Chem.* **367** (1994) 123.
13. M.W. Verbrugge and B.J. Koch, *J. Electrochem. Soc.* **141** (1994) 3053.
14. J.J. Xu and G.C. Farrington, *J. Electrochem. Soc.* **145** (1998) 744.
15. L. Christie, A.M. Christie and C.A. Vincent, *J. Electrochem. Soc.* **2** (1999) 187.
16. J. Newman, 'Electrochemical Systems,' second edition, Prentice-Hall, Englewood Cliffs, New Jersey (1991).
17. K.B. Oldham, *J. Electroanal. Chem.* **122** (1981) 1.
18. K. Aoki and J. Osteryoung, *J. Electroanal. Chem.* **122** (1981) 19.
19. K. Aoki and J. Osteryoung, **160** (1984) 335.
20. J. Barthel, H.-J. Gores and G. Schmeer, *Ber. Bunsenges. Phys. Chem.* **83** (1979) 911.
21. H.-J. Gores and J. Barthel, *J. Solution Chem.* **9** (1980) 939.
22. R. Jasinski, 'Electrochemistry and Application of Propylene Carbonate.' In Advances in Electrochemistry and Electrochemical Engineering, (edited by P. Delahay and C.W. Tobias) Vol. 8, Wiley-Interscience, New York, NY (1971).
23. S.G. Meibuhr, *J. Electrochem. Soc.* **117** (1970) 56.
24. B. Scrosati and S. Megahed, 'Rechargeable Lithium-Ion (Rocking Chair) Batteries for Consumer, Electronic, Military, and Aerospace Applications,' an Electrochemical Society Short Course, The Electrochemical Society (1993).
25. R.J. Blint, *J. Electrochem. Soc.* **142** (1995) 698.
26. Y. Ma, M. Doyle, T.F. Fuller, M.M. Doeff, L.C. De Jonghe and J. Newman, *J. Electrochem. Soc.* **142** (1995) 1859.
27. J. Sullivan, D. Hansen and R. Keller, *J. Electrochem. Soc.* **117** (1970) 779.
28. W.M. Hedges and D. Pletcher, *J. Chem. Faraday Trans. 1* **82** (1986) 179.
29. C.G. Zoski and A.M. Bond, *Anal. Chem.* **62** (1990) 37.
30. A.C. Michael, R.M. Wightman and C.A. Amatore, *J. Electroanal. Chem.* **267** (1989) 33.
31. M.W. Verbrugge and D.R. Baker, *J. Phys. Chem.* **96** (1992) 4572.
32. C.A. Amatore and B. Fosset, *J. Electroanal. Chem.* **328** (1992) 21.
33. P.N. Pintauro and D.N. Bennion, *Ind. Eng. Chem. Fundam.* **23** (1984) 234.
34. K.H. Keller, E.R. Canales and S.I. Yum, *J. Phys. Chem.* **75** (1971) 379.
35. M.W. Verbrugge, *J. Electrochem. Soc.* **136** (1989) 417.
36. M.W. Verbrugge and R.F. Hill, *Electrochim. Acta* **37** (1992) 221.
37. Y. Marcus, '*Ion Solvation*,' Wiley, New York, NY (1985). (See chapter 6, 'Ion solvation in nonaqueous solvents.')